EASR

Engineering and Applied Science Research

https://www.tci-thaijo.org/index.php/easr/index

Published by the Faculty of Engineering, Khon Kaen University, Thailand

Development of a non-thermal gliding-arc discharge reactor for biomass tar treatment

Kittikorn Sasujit[1)], Natthawud Dussadee[2)] and Nakorn Tippayawong*[1)]

[1)]Department of Mechanical Engineering, Faculty of Engineering, Chiang Mai University, Chiang Mai 50200, Thailand
[2)]School of Renewable Energy, Maejo University, Chiang Mai 50290, Thailand

Received 29 December 2018
Revised 15 March 2019
Accepted 20 March 2019

Abstract

Non-thermal plasma technology is an interesting method for removal of tar from gasified biomass. In this study, AC gliding-arc reactors with a reverse vortex flow configuration were developed for biomass tar treatment. Successful generation of plasma discharge was obtained at high volume flows of treated gas. Preliminary experimental results showed that the onset of electric discharge occurred at about 10 kV. A large number of plasma discharges was evident. For our developed prototype, electric power input, total gas feed rate, and various carrier gases (Air, N_2, N_2+$C_{10}H_8$) were adjusted to investigate their effects on the discharge phenomena. The reverse vortex flow gliding arc discharges showed high residence times for potential chemical reactions inside the reactor. From preliminary tests, maximum removal efficiency of a representative tar compound of more than 93% was found, at an energy utilization efficiency of about 30 g/kWh.

Keywords: Non-thermal plasma, Reverse vortex flow, Gliding arc, Tar removal

1. Introduction

Recently, biofuels and biomass have received considerable interest as important renewable energy sources. In terms of simple applications and high energy efficiency, gasification is a thermal conversion technique that can convert biomass into fuel gas or producer gas [1-4]. However, tar, particulate matter, alkali metals and ash are also present as impurities in the fuel gas [5]. Tar is a condensable mixture of aromatic and polycyclic aromatic hydrocarbons. Tar removal is necessary for successful commercialization of biomass gasification [6]. Tar in the producer gas presents significant operational challenges to a gasifier system and problems in engines such as blockage of fuel lines and heat exchanger system, leading to high maintenance costs [7]. The composition of tar depends on the reaction temperature, biomass feedstock, and the type of reactor. The main component of tar from biomass gasification was identified as polycyclic aromatic hydrocarbons including naphthalene and anthracene compounds [8].

Non-thermal plasma technology is an interesting option for decomposition of volatile organic compounds because of its ease of operation and compact design downstream [9]. Non-thermal plasma generates a variety of reactive species (electrons, radicals and excited species), which can interact with tar compounds [10]. There are many types of non-thermal plasma reactors, but a reverse vortex flow (RVF) gliding arc (GA) plasma reactor, depicted schematically in Figure 1, has recently gained enormous interest. It was originally used for decomposition and reforming of hydrocarbons [11]. Transitional GA discharge using a cylindrical geometry was developed in a RVF. It can provide excellent thermal insulation of active species generated by the plasma from the cylindrical wall, significantly reducing energy loss to the surroundings, and thus increasing its energy efficiency [12-13]. The advantages of the RVF-GA include a large plasma region, less heat dissipation, and abundant active species (electrons, ions, and radicals). It enables long residence times for a higher degree of completion of chemical reactions, and provides very good convective cooling in the discharge zone. Thus, the RVF-GA discharge offers the capability to both increase specific power input and ensure a uniform treatment of the gas. Although the GA discharge has an excellent energy density for chemical reactions and desirable retention time of gas, it has not yet been used for treatment of a biomass tar from gasification [13-15]. In this work, the development of a RVF-GA discharge reactor was carried out. Characteristics of the electric arc and images of plasma flame using various carrier gases were investigated. Preliminary tar removal efficiency was also evaluated.

2. Design of a reverse vortex flow gliding-arc reactor

2.1 RVF-GA reactor

A schematic of the RVF-GA reactor is illustrated in Figure 2. The RVF-GA reactor consists of a top plate (A), bottom plate (B), quartz tube (C), tangential gas inlet or swirl

*Corresponding author.
Email address: n.tippayawong@yahoo.com
doi: 10.14456/easr.2019.20

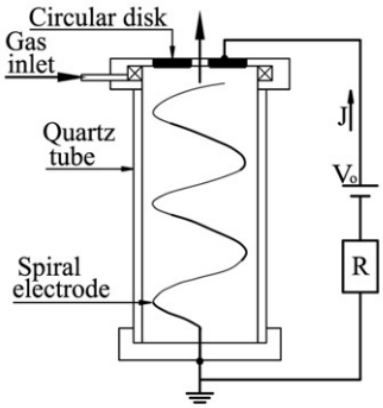

Figure 1 Schematic diagram of the reverse vortex flow gliding arc reactor [11, 16]

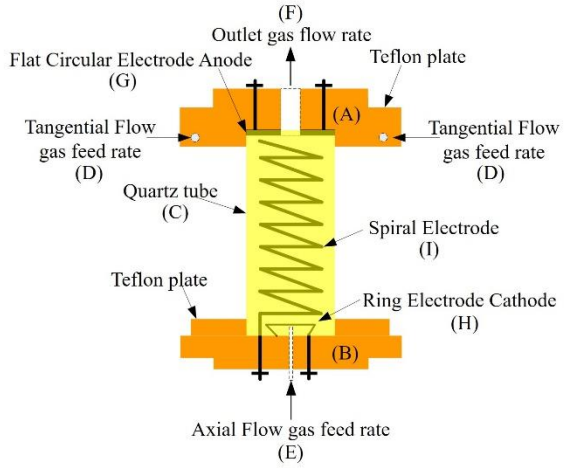

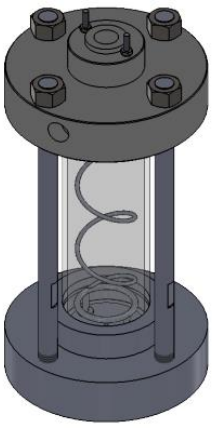

Figure 2 Schematic of the reverse vortex flow gliding arc reactor

generator (D), axial gas inlet (E), outlet gas discharge (F), circular electrode (G), ring electrode (H), and spiral electrode (I). Electrodes made of stainless steel were separated by the swirl generator and connected with rods threaded through four holes. The inlet gas was injected into the reactor through the generator, and a swirling flow was formed between the electrodes. The reaction chamber was made from a quartz tube with a length of 60 mm and an inner diameter of 40 mm. The design dimensions and gas flow rates that could

Figure 3 The prototype of the reverse vortex flow gliding arc discharge reactor

sustain arc propagation were based on values derived from the literature [13, 17]. The inlet gas entered the reactor tangentially through the swirl generator and exited at the upper end of the reactor. The circular electrode was flat with an inner diameter of 12.6 mm and outer diameter of 33.3 mm. The ring and spiral electrodes were made of stainless steel wire that was about 1.1 mm in diameter. The top and bottom plates were made of Teflon. An arc was produced at the center of the reactor. The roots of the GA were connected to the outlet and the ground electrode. The length of the arc was kept constant under a discharge stability condition.

The prototype of the RVF- GA system is shown in Figure 3. The geometry was similar to a tornado GA system [11]. The HV electrode was a stainless wire with a helical profile fixed in a stainless steel holder. The size of the prototype was 150 mm x 120 mm. It weighed approximately 1.2 kg.

2.2 Power supply and electrode design

The power supply used was an AC neon transformer (LEIP EX230A 15N) connected to a 220 V, 50 Hz electrical supply. The resistance was 180 Ω to control the current and flexibly vary the power characteristics of the RVF- GA discharge. The maximum current and voltage were 30 mA and 15 kV [18-19]. The power supply for this experiment is shown in Figure 4. It was a low-cost, simple design that was developed especially for the tar treatment application.

The electrodes of the RVF-GA discharge consisted of a circular disk electrode and a spiral electrode. The circular disk electrode, which acted as the anode, was positioned at the top of the cylindrical reactor. It was made of stainless steel, with an inner diameter of 12.6 mm, outer diameter of 33.3 mm and thickness of 1.5 mm. The spiral electrode was used as a cathode and it was placed inside the cylindrical reactor with the quartz tube. The narrowest gap between the two electrodes

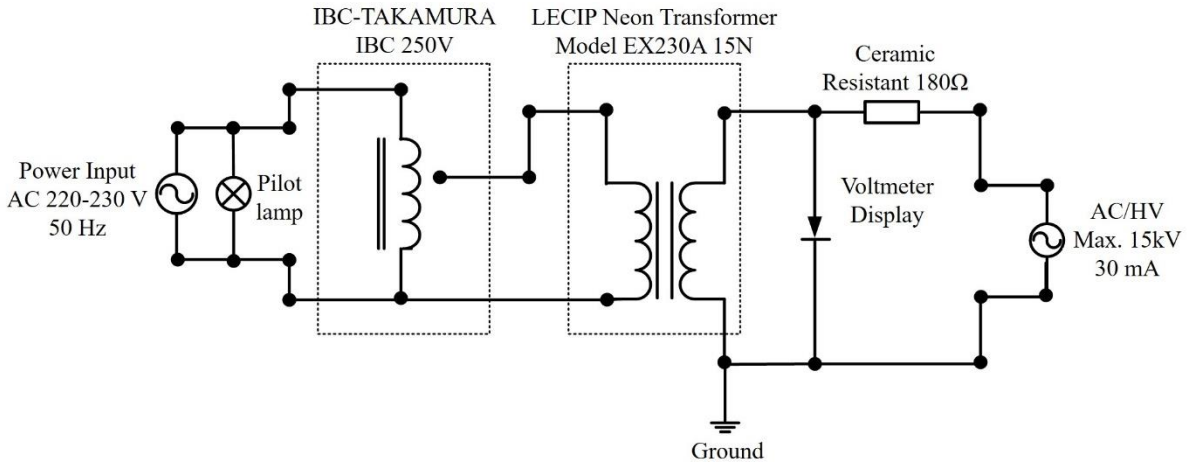

Figure 4 A schematic circuit diagram of the AC high voltage power supply

for arc ignition was 3 mm. It caused a minimum disturbance to the gas flow rate inside the reactor. The initial breakdown started between the circular disk electrode and the tip of the spiral electrode. The opposite end of the spiral electrode had a ring electrode that was smaller in diameter than the spiral diameter to provide stability when the arc was fully elongated.

2.3 Gas flows

The RVF-GA reactor was made from a quartz tube, where the upper part of the tube acted as a swirl generator with a tangential flow at the inlet of the cylinder. The gas outlet of the reactor was at the same end as the swirl generator. An axial inlet was located at the bottom of the reactor, providing flexibility for additional carrier gas. Generally, the GA discharge was driven using a tangential gas flow of 7 to 12 L/min through four injectors on the upper part of the reactor and injection of axial gas at a flow of 0.8 to 1.5 L/min at the bottom of the reactor. The retention time was adjustable by varying the total gas flow rate [14, 20].

2.4 Performance indices

The performance of the RVF-GA reactor was evaluated based on the decomposition efficiency and energy utilization. These parameters were calculated as follows:

2.4.1 Decomposition efficiency

The decomposition efficiency (DE), which explains the degree of naphthalene decomposition in gas, was calculated as:

$$DE(\%) = \frac{[VC]_{inlet} - [VC]_{outlet}}{[VC]_{inlet}} \times 100 \quad (1)$$

Where $[VC]_{inlet}$ is the input naphthalene concentration (mg/m^3) and $[VC]_{outlet}$ is the outlet naphthalene concentration (mg/m^3).

2.4.2 Energy utilization efficiency

The energy utilization efficiency (η_e), refers to the decomposed mass of tar divided by the energy required for its breakdown. It is calculated as:

$$\eta_e(g/kWh) = \frac{Q \times \{[VC]_{inlet} - [VC]_{outlet}\}}{IP} \quad (2)$$

where Q is the gas feed rate (m^3/h) into the reactor and IP is the plasma input power (kW).

2.4.3 Specific energy input

The specific energy input (SEI), the ratio of the input energy to the gas feed rate, was calculated as:

$$SEI(kWh/m^3) = \frac{IP}{Q} \quad (3)$$

3. Experimental test setup

Figure 5 shows a schematic diagram of the experimental setup, consisting of the RVF-GA reactor, model tar generator, power supply, tar sampling and electrical measurement system. The inlet gas was injected into the reactor through four tangential holes to form a swirling flow. The arc was initially ignited at the narrowest gap and then moved to the upper part of the reactor. Discharges occurred between the ring and spiral electrodes and rotated to the upper part. The arc discharge zone had an approximate height of 20 to 30 mm. The HV power source was connected to the RVF-GA reactor to generate plasma and a 180 Ω resistance that was used as a current limiter. The electrical parameters were measured using an oscilloscope (GW-INSTEK GDS-1052-U) monitoring the dynamic behavior of the arc, a HV probe (Model 80K-40, Fluke, Germany), and a low current probe (Model i1000s, Fluke, Germany). The power supply can provide 450 W to the GA plasma reactor.

4. Test results and discussion

4.1 Electrical properties

In this experiment, the electrical power source was supplied at 50 Hz, 220-230 V to generate the required high voltage. The discharge current was limited using resistors. The HV power source was adjusted using a variable voltage transformer. Input/ output characterization of the power supply employed in this research is shown in Figure 6. The results show a relationship between the input voltage and

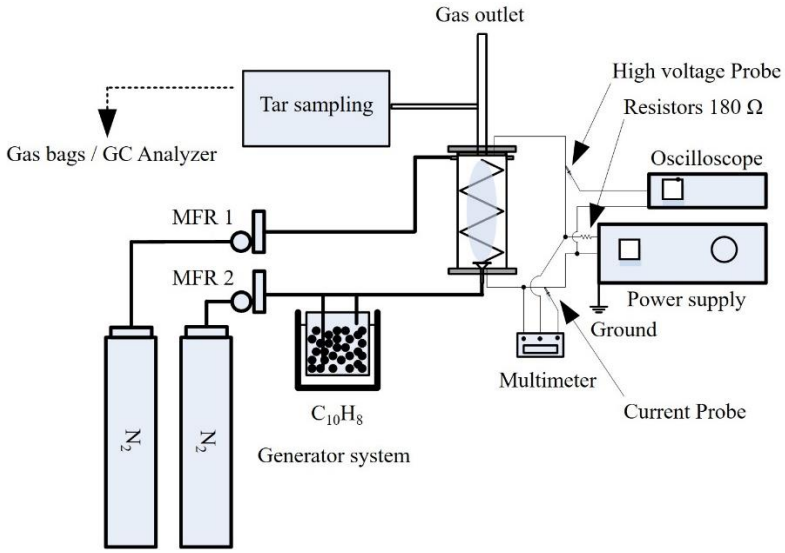

Figure 5 Experimental setup for plasma treatment of tar testing

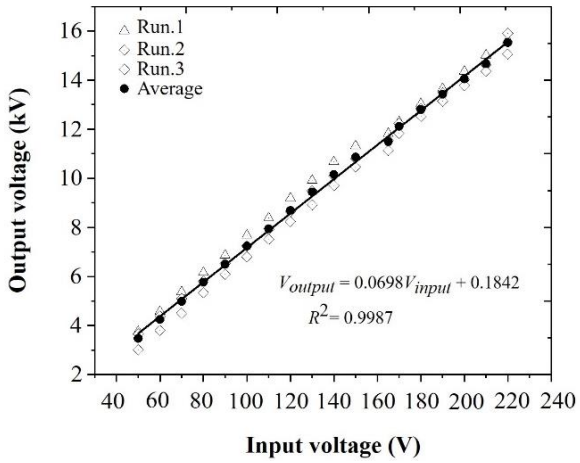

Figure 6 Effect of input voltage on output high voltage of the power supply

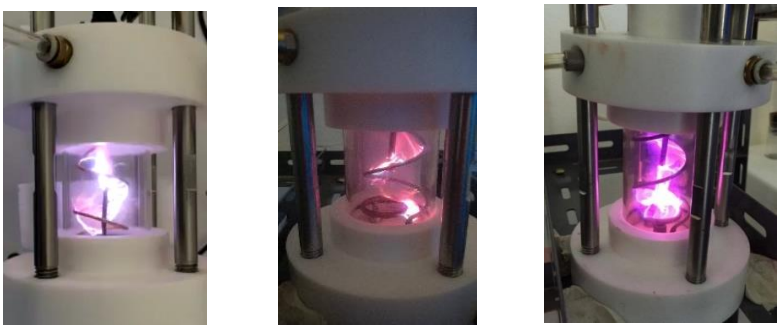

(a) Air (b) N_2 (c) $N_2 + C_{10}H_8$

Figure 7 Images of RVF-GA discharges using various carrier gases

HV output for an adjustable range of input voltages (50 to 220 V), generating HV outputs of 2 to 15 kV. The power supply exhibited a linear relation between the input and output ($R^2 = 0.9987$).

4.2 RVF-GA discharge phenomenon

Figure 7 shows discharges of the RVF-GA reactor and arc images with various carrier gases (air, nitrogen, and nitrogen mixed with traces of a naphthalene compound). The characteristics of an elongated plasma flame color inside the reactor are clearly seen. The white color of the plasma flame in Figure 7(a), the reddish pink color in Figure 7(b), and the violet color in Figure 7(c) were clearly seen when using air, nitrogen, and nitrogen as carrier gases, respectively, mixed with traces of a naphthalene compound [12, 21]. All experiments were controlled at a HV of about 10-12 kV with a total gas flow rate of 60-80 L/min. These observations

(a) Voltage = 11 kV (Power = 333 W) (b) Voltage = 13 kV (Power = 394 W) (c) Voltage = 15 kV (Power = 445 W)

Figure 8 Effect of applied voltage and power on plasma flame phenomena

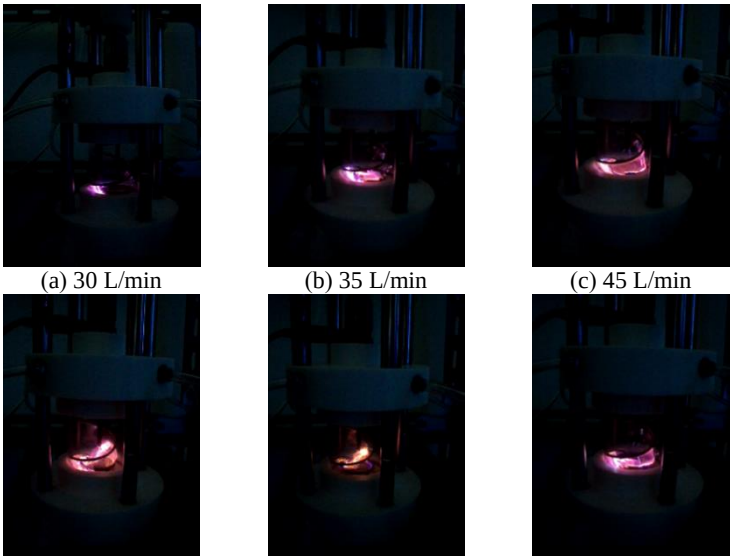

(a) 30 L/min (b) 35 L/min (c) 45 L/min

(d) 55 L/min (e) 65 L/min (f) 75 L/min

Figure 9 Effect of total gas flow rate on plasma flame phenomena

are similar to those previously reported [22]. It was found that the colors of the plasma varied depending on the type of medium gas used and the energy density for excitation of the carrier gas to form a plasma flame. Excited nitrogen gas molecules were pink and red. The pink or violet plasma flames indicated a higher energy density than red or orange [23].

Figure 8 compares the effect of electrical power on the characteristics of the plasma flame by varying applied HV between 11, 13 and 15 kV at a fixed total gas feed rate of 40 L/ min using nitrogen as a carrier gas mixed with a naphthalene compound (the concentration of naphthalene was about 4,300 mg/m^3). It was seen that plasma discharge can be achieved for all experimental conditions considered. An increase in the electric power appeared to enhance the electric arc at the gap between the anode and cathode electrodes. Gas molecules were ionized into high energy ions and radicals under the electric field. The arc volume was larger with increasing applied power. Heat dissipation was expected to increase progressively. Eventually, the electric arc connected the anode at the top and the cathode on the bottom, and steady vortex GA plasma was obtained. The central region of the reactor was fully engulfed in a plasma region, sufficient for chemical reactions [17, 20].

Likewise, Figure 9 shows the effect of the total gas flow rate between 30 to 75 L/min on the characteristics of the plasma flame with an inlet naphthalene concentration of about 4,300 mg/m^3 and a HV supply of 10 to 15 kV. It was found that the initial discharge of the reactor occurred at an input voltage of 10 kV and increased as the tangential flow rate adversely affected the plasma flames. The plasma flame was observed to be slightly shorter with an increased tangential flow rate. Moreover, the proportion between tangential and axial flow rates seemed to affect the plasma flame zone.

4.3 Preliminary tests of naphthalene removal

Figure 10 shows the preliminary test results of naphthalene decomposition by GA discharge. The applied HV was varied between 11 to 15 kV at a fixed inlet naphthalene concentration of 4,300 mg/m^3. The highest and lowest input powers used were 440 and 315 W, respectively. The naphthalene decomposition was found to be 89 to 93%, and slightly decreased with voltage. It was also shown that the RVF-GA should be operated with an input voltage of 11 kV to ensure good stability with a low specific energy input of 0.254 kWh/m^3. At higher voltages, the specific energy input was greater and risked becoming unstable. The production of active species with some decomposition selectivity may change with variation of the input voltage, modulating the decomposition efficiency [24].

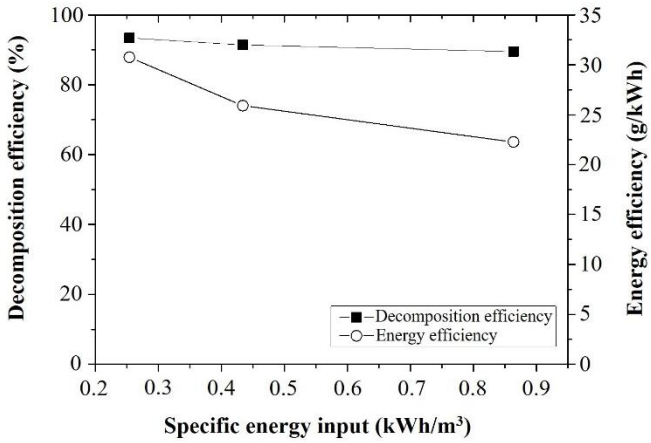

Figure 10 Effect of specific energy input on decomposition efficiency and energy efficiency

Additionally, the electric transfer between electrodes became higher with increasing input voltage.

5. Concluding remarks

A prototype of a RVF-GA reactor for decomposition of tar from biomass gasification was developed. Preliminary tests to study the effect of the electric power, variation in carrier gases, and total gas flow rate on plasma generation were done. A RVF-GA discharge with a high residence time is attractive for many applications such as volatile compound decomposition, biomass tar destruction, methane reforming, and inactivation of *E. coli* in water. RVF-GA discharge demonstrated excellent results in preliminary experiments, providing good plasma/ gas contact and keeping most of generated active species in the flow for effective plasma-chemical reactions. From the findings, the plasma flame in the reaction chamber was controlled under various conditions, including mass flow ratio, residence time, type of carrier gas, and total gas feed rate. The developed GA discharge technology may be applied to tar destruction. From preliminary tests, a high decomposition efficiency of more than 93% was achieved. Nonetheless, further characterization of plasma using optical emission spectroscopy [25] should be carried out. Computational fluid dynamics of the gas flow rate in the cylindrical tube reactor will be useful in visualizing the effect of the gas mixing and flow on the performance of the plasma reactor.

6. Acknowledgements

The authors would like to thank Chiang Mai University and National Research Council of Thailand for support.

7. Nomenclature and Greek letters

AC	alternating current
CFD	computational fluid dynamics
eV	electron volt
GA	gliding arc
HV	high voltage
NTP	non-thermal plasma
OES	optical emission spectroscopy
PTTFE	polytetrafluoroethylene
RVF	reverse vortex flow
3D	three dimensional
Ω	ohm
η_e	energy utilization efficiency

8. References

[1] Punnarapong P, Promwungkwa A, Tippayawong, N. Development and performance evaluation of a biomass gasification system for ceramic firing process. Energy Procedia. 2017;110:53-8.

[2] Wongsiriamnuay T, Kunnang N, Tippayawong N. Effect of operating conditions on catalytic gasification of bamboo in a fluidized bed. Int J Chem Eng. 2013; 2013:1-9.

[3] Wongsiriamnuay T, Tippayawong N. Product gas distribution and composition from catalyzed gasification of mimosa. Int J Renew Energ Res. 2012; 2(3):363-8.

[4] Xu B, Xie J, Zhan H, Yin X, Wu C, Liu H. Removal of toluene as a biomass tar surrogate in a catalytic non-thermal plasma process. Energ Fuel. 2018;32(10):10709-19.

[5] Sasujit K, Dussadee N, Homdoung N, Ramaraj R, Kiatsiriroat T. Waste- to- energy: producer gas production from fuel briquette of energy crop in Thailand. Int Energ J. 2017;17(1):37-46.

[6] Capareda S. Introduction to biomass energy conversions. New York: CRC press; 2013.

[7] McKendry P. Energy production from biomass (part 3): gasification technologies. Bioresource Technol. 2002;83(1):55-63.

[8] Hernández JJ, Ballesteros R, Aranda G. Characterisation of tars from biomass gasification: Effect of the operating conditions. Energy. 2013;50 (1):333-42.

[9] Jin Q, Jiang B, Han J, Yao S. Hexane decomposition without particle emission using a novel dielectric barrier discharge reactor filled with porous dielectric balls. Chem Eng J. 2016;286:300-10.

[10] Yan K, Heesch EJMv, Pemen AJM, Huijbrechts PAHJ, Gompel FMv, Leuken Hv. A high-voltage pulse generator for corona plasma generation. IEEE Trans Ind Appl. 2002;38(3):866-72.

[11] Fridman A. Plasma chemistry. Cambridge: Cambridge University Press; 2008.

[12] Zhu J, Kusano Y, Li Z. Optical diagnostics of a gliding arc discharge at atmospheric pressure. In: Parker M, editor. Atmospheric pressure plasmas: processes, technology and applications. New York: Nova Science Publishers; 2016.

[13] Piavis W, Turn S. An experimental investigation of reverse vortex flow plasma reforming of methane. Int J Hydrogen Energ. 2012;37(22):17078-92.
[14] Xu G, Ding X. Optimization geometries of a vortex gliding-arc reactor for partial oxidation of methane. Energy. 2012;47(1):333-9.
[15] Kalra CS, Kossitsyn M, Iskenderova K, Chirokov A, Cho YI, Gutsol A, et al. Electrical discharges in the reverse vortex flow–tornado discharges. Electronic Proceedings of 16th International Symposium on Plasma Chemistry; 2003 Jun 22-27; Taormina, Italy. Bari: University of Bari; 2003.
[16] Kim HS, Wright KC, Hwang IW, Lee DH, Rabinovich A, Fridman A, et al. Concentration of hydrogen peroxide generated by gliding arc discharge and inactivation of *E. coli* in water. Int Comm Heat Mass Tran. 2013;42:5-10.
[17] Ren Y, Li X, Lu S, Yan J. Generation process and electric arc motion characteristics of DC vortex gliding arc plasma. IEEE Trans Plasma Sci. 2014;42(10):2702-3.
[18] Thanompongchart P, Tippayawong N. Experimental investigation of biogas reforming in gliding arc plasma reactors. Int J Chem Eng. 2014;2014:1-9.
[19] Tippayawong N, Inthasan P. Investigation of light tar cracking in a gliding arc plasma system. Int J Chem React Eng. 2010;8(1):1-15.
[20] Ren Y, Li X, Lu S, Yan J. Solid hazardous waste treatment and material modification by vortex gliding arc plasma. IEEE Trans Plasma Sci. 2014;42(10):2750-1.
[21] Yu L, Li X, Tu X, Wang Y, Lu S, Yan J. Decomposition of naphthalene by DC gliding arc gas discharge. J Phys Chem A. 2009;114(1):360-8.
[22] Ren Y, Li X, Wu A, Lu S, Yan J. Operation patterns and spectrum characteristics of DC and AC rotating gliding arc plasma. IEEE Trans Plasma Sci. 2014;42(10):2700-1.
[23] Chen FF. Introduction to plasma physics. New York: Springer Science & Business Media; 2012.
[24] Ren Y, Li X, Ji S, Lu S, Buekens A, Yan J. Removal of gaseous HxCBz by gliding arc plasma in combination with a catalyst. Chemosphere. 2014;117:730-6.
[25] Zhang H, Li L, Li X, Wang W, Yan J, Tu X. Warm plasma activation of CO_2 in a rotating gliding arc discharge reactor. J CO_2 Util. 2018;27:472-9.